Diffraction of Visible Light by Ordered Monodisperse Silica−Poly(methyl acrylate) Composite Films

Jagdish M. Jethmalani and Warren T. Ford*

Department of Chemistry, Oklahoma State University, Stillwater, Oklahoma 74078

Received January 30, 1996. Revised Manuscript Received May 1, 1996[⊗]

Composites of ordered colloidal crystals of amorphous monodisperse silica particles in amorphous poly(methyl acrylate) (PMA) films selectively Bragg diffract visible light. The 153 nm diameter colloidal silica particles coated with 3-(trimethoxysilyl)propyl methacrylate form colloidal crystals in methyl acrylate (MA) monomer, and the crystal order is locked into place by polymerization of the MA. Bragg diffraction from the films is detected spectrophotometrically as narrow peaks of low percent transmission of visible light normal to the film plane. The diffraction wavelength is tuned by varying the *d* spacing of the crystal lattice and by varying the Bragg angle. Variation in the lattice spacing is achieved via the particle size or particle concentration, uniaxial stretching of the composite, and swelling the composite with monomers such as styrene or MA followed by photopolymerization of the imbibed monomers. Films that diffract from 434 to 632 nm have been prepared.

Introduction

Silica−polymer composites often have improved mechanical and thermal properties relative to the unfilled polymer.[1] In all previous composites, the silica has been present as randomly distributed colloidal silica or silica fiber. The colloidal silica may be preformed or prepared in situ by either basic or acidic hydrolysis and condensation of tetraethyl orthosilicate (TEOS) or tetramethyl orthosilicate (TMOS).[1] Previously, we have trapped the ordered monodisperse amorphous colloidal silica in poly(methyl methacrylate) (PMMA) films.[2]

Monodisperse charged colloidal particles in aqueous and nonaqueous dispersions can self-assemble into a three-dimensional lattice known as a colloidal crystal. Several factors govern the formation and orientation of colloidal crystals, such as the size, surface charge, and concentration of particles and the ionic strength of the medium.[2−5] The crystals are generally face-centered cubic (fcc) at high particle volume fractions and low surface charges, and body-centered cubic (bcc) at low particle volume fractions and high surface charges.[3,6−8] Since the lattice spacings usually exceed 100 nm, the dispersions efficiently diffract visible light according to Bragg eq 1,[2−13] where λ is the wavelength of diffracted

$$\lambda = 2dn \sin \theta \qquad (1)$$

light, d is the interplanar spacing, n is the refractive index of the dispersion, and θ is the Bragg angle. Consequently, colloidal crystalline materials may be used in optical devices such as rejection filters, limiters, and switches.[10−13] Our silica−polymer composite films are more robust than any previous colloidal crystalline materials. Ordered silica−PMMA films are thermoplastic like the parent polymer, and the narrow diffraction peaks in spectra of the films are retained even after heating to 150 °C.[2] The aim of the research reported here is to create films that will allow tuning of the diffraction wavelength by stretching and swelling.

Diffraction wavelengths from liquid colloidal dispersions have been tuned by varying the particle size,[5] particle concentration,[5,9] and Bragg angle.[10−12] A gradient of particle concentration, and consequently of diffraction wavelength, can be created by particle sedimentation.[13] The diffraction wavelengths of polyacrylamide gels containing colloidal crystals of polystyrene latexes have been tuned by mechanical stress.[14,15]

[⊗] Abstract published in *Advance ACS Abstracts,* July 15, 1996.

(1) (a) Iler, R. K. *The Chemistry of Silica*; Wiley: New York, 1979; pp 582−588. (b) Sanchez, C.; Ribot, F. *New J. Chem.* **1994**, *18*, 1007. (c) Mark, J. E., Lee, C. Y.-C., Biancone, P. A., Eds. *Hybrid Organic-Inorganic Composites*; ACS Symposium Series 585; American Chemical Society: Washington, DC, 1995. (d) Landry, C. J. T.; Coltrain, B. K.; Brady, B. K. *Polymer* **1992**, *33*, 1486. (e) Pope, E. J. A.; Asami, M.; Mackenzie, J. D. *J. Mater. Res.* **1989**, *4*, 1018.

(2) (a) Sunkara, H. B.; Jethmalani, J. M.; Ford, W. T. *Chem. Mater.* **1994**, *6*, 362. (b) Sunkara H. B.; Jethmalani J. M.; Ford, W. T. *ACS Symp. Ser.* **1995**, *585*, 181.

(3) (a) Carlson, R. J.; Asher, S. A. *Appl. Spectrosc.* **1984**, *38*, 297. (b) Dhont, J. K. G.; Smits, C.; Lekkerkerker, H. N. W. *J. Colloid Interface Sci.* **1992**, *152*, 386.

(4) (a) Kesavamoorthy, R. Tandon, S.; Xu, S.; Jagannathan, S.; Asher, S. A. *J. Colloid Interface Sci.* **1992**, *153*, 188. (b) Okubo, T. *Langmuir* **1994**, *10*, 1695.

(5) (a) Hiltner, P. A.; Krieger, I. M. *J. Phys. Chem.* **1969**, *73*, 2386. (b) Okubo, T. *Colloid Polym. Sci.* **1993**, *271*, 190. (c) Okubo, T. *J. Chem. Soc., Faraday Trans. 1* **1986**, *82*, 3163. (d) Okubo, T. *J. Chem. Soc., Faraday Trans. 1* **1986**, *82*, 3175.

(6) Clark, N. A.; Hurd, A. J.; Ackerson, B. J. *Nature* **1979**, *281*, 57.

(7) (a) Rundquist, P. A.; Photinos, P.; Jagannathan, S.; Asher, S. A. *J. Chem. Phys.* **1989**, *91*, 4932. (b) Spry, R. J.; Kosan, D. J. *Appl. Spectrosc.* **1986**, *40(6)*, 782. (c) Monovoukas, Y.; Gast, A. P. *Langmuir* **1991**, *7*, 460.

(8) Monovoukas, Y.; Gast, A. P. *Phase Transitions* **1990**, *21*, 183.

(9) Krieger, I. M.; Hiltner, P. A. *Polymer Colloids Proceedings*; ACS Symposium on Polymer Colloids; Fitch, R., Ed.; Plenum Press: New York, 1971; p 63.

(10) (a) Asher, S. A.; Kesavamoorthy, R.; Jagannathan, S.; Rundquist, P. A. *Nonlinear Opt. III* **1992**, *SPIE Vol. 1626*, 238. (b) Asher, S. A. U.S. Patent 4,627,689, 1986. (c) Asher, S. A.; Jagannathan S. U.S. Patent 5,281,370, 1994.

(11) Flaugh, P. L.; O'Donnell, S. E.; Asher, S. A. *Appl. Spectrosc.* **1984**, *38*, 847.

(12) Asher, S. A.; Flaugh, P. L.; Washinger, G. *Spectroscopy* **1986**, *1*, 26.

(13) (a) Okubo, T. *Prog. Polym. Sci.* **1993**, *18*, 481. (b) Okubo, T. *Colloid Polym. Sci.* **1993**, *271*, 873. (c) Okubo, T. *J. Chem. Phys.* **1987**, *86*, 2394. (d) Okubo, T. *J. Chem. Phys.* **1988**, *88*, 6581.

(14) (a) Asher, S. A.; Holtz, J.; Liu, L.; Wu, Z. *J. Am. Chem. Soc.* **1994**, *116*, 4997. (b) Panzer, H. P., Giovanni, L.; Cohen, M. L.; Yen, W. S. U.S. Patent 5,338,492, 1994.

S0897-4756(96)00065-8 CCC: $12.00

Here we show that the diffraction wavelength decreases by photopolymerizing silica−MA (MA = methyl acrylate) dispersions to form polymer composites and by uniaxially stretching the composites, and that the wavelength increases by swelling the silica−PMA composites with monomers.

Experimental Section

TEOS and TPM were vacuum distilled, and absolute ethanol was distilled shortly before use. Ammonium hydroxide, MA, and 2,2-dimethoxy-2-phenylacetophenone (DMPA) were used as obtained. Styrene was distilled under vacuum and stored at 4 °C. Dialysis employed 22 mm diameter Spectra-Por cellulose ester membrane tubing (Spectrum Catalog no. 132130) with a molecular weight cutoff of 50 000. The polarizing microscopic studies were done on a Nikon OPTIPHOT-POL polarizing microscope. The UV−visible spectra were obtained with the incident light normal to the plane of the glass cell on a Hewlett-Packard 8452A spectrophotometer with a diode array detector having a resolution of 2 nm. The cell was mounted on a stage that rotates around axes parallel and normal to the light. Rotation about the vertical axis was carried out in 2° steps.

TPM−Silica Particles. Colloidal silica was prepared from TEOS, and TPM was grafted to the particles as described before.[2,16,17] The number average particle diameter was 153 nm by transmission electron microscopy (TEM), with a polydispersity (standard deviation/mean) of 0.07 and was 171 nm by dynamic light scattering.[18] The dispersion of TPM−silica in ethanol was transferred to methanol by dialysis[2,19] and concentrated to a 56 wt % particle dispersion.

Cell Preparation. Microscope slides were silylated overnight by immersion in a solution of 10% dichlorodimethylsilane in cyclohexane, washed with cyclohexane and water, and dried at 110 °C. To make a cell, one plain slide and one with two drilled holes at one end were wiped clean with Kimwipes and a lint-free brush, sandwiched and clamped around two Teflon spacers of 132 μm thickness each, and sealed on two sides and one end using Devcon 5-Minute epoxy. After the epoxy dried, the Teflon spacers were removed, and the remaining end was sealed with the epoxy, leaving the holes open for filling the dispersions.

TPM−Silica in MA Dispersion. A concentrated dispersion of 48 wt % TPM−silica in MA was made by dialyzing the methanolic dispersion with MA. After five replacements of MA, the dispersion contained <1% methanol as analyzed by ^{1}H NMR. Silica contents were analyzed by measuring 250 μL of the concentrated dispersion into a tared aluminum pan, air drying, oven-drying at 90 °C, and weighing the dried particles.

The desired particle concentrations of 35, 40, and 45 wt % were made by diluting the 48 wt % dispersion with more MA. For example, a MA dispersion of 40 wt % particles and volume 0.6 mL was prepared from 0.5 mL of 48 wt % dispersion and 0.1 mL of MA in a vial which contained 9.0 mg (~0.2 wt % to the monomer) of photoinitiator, DMPA. The DMPA was dissolved by vortex mixing for a minute and syringed into the cell through the holes. A cover-slip with Duro Quick-Gel glue was used to seal the holes quickly, followed by sealing with 5-Minute epoxy. The cell was kept horizontal at 25 ± 1 °C for crystallization and growth. Visible spectra were obtained with the cells vertical. The orthoscopic images between crossed polarizers were observed with the plane of the cell at an angle of 40−55° to the light beam of a polarizing microscope.

Scheme 1

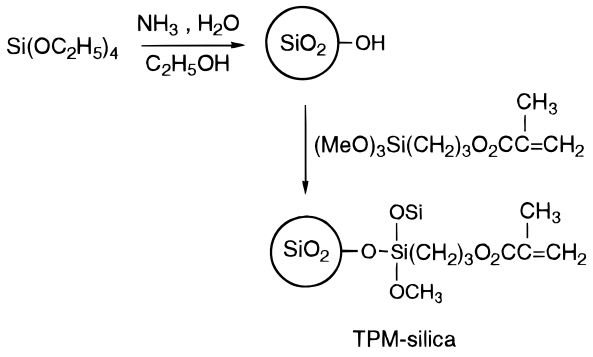

TPM-silica

Photopolymerization. After 6−8 h, when a narrow peak was observed in the spectrum, the cell was placed horizontally in a water bath at 27 ± 1 °C and irradiated for 3.5−4 h using a medium-pressure 450 W Hg lamp. The films were removed from the cells for stretching and swelling experiments.

Stretching of PMA Composite Films. The films were stretched with a homemade device having clamps attached to a micrometer with a least count of 0.001 in. The initial distance between the clamps holding the film was 1.0 cm. The transmission spectra before, during, and after stretching were observed with the film normal to the incident light beam. The spectrum and the length of the film were measured after each stretch until only a weak peak remained in the spectrum. After release of stress, the films returned to their original dimensions in 2−4 h.

Swelling of PMA Composite Films. To a 35 wt % TPM−silica−PMA composite film between glass slides held apart by two 132 μm pieces of Teflon at each end, a solution of 1 wt % DMPA in MA monomer was transferred by capillary action. The sample was kept horizontally above MA monomer in a closed glass dish, while MA diffused into the composite. During swelling, the sample was removed from the dish periodically, and the visible spectrum was measured. More MA with 1 wt % DMPA was added between the slides, and after further swelling, the excess MA was removed by wiping with Kimwipes, and the film was irradiated for 3−4 h. The swollen and repolymerized film was slightly thicker than the two Teflon spacers.

Scanning Electron Microscopy (SEM). Composite films were microtomed normal to the surface, followed by coating the surfaces with Au−Pd under vacuum. The samples were examined on a JEOL JSM-35U scanning electron microscope at 25 kV and 20 000 magnification.

Results

Colloidal Crystals in MA. Scheme 1 gives the chemical structure of the TPM−silica particles. Dispersions of 35, 40, and 45 wt % 153 nm diameter TPM−silica in MA in silanized glass cells were placed horizontally in an oven at 25 °C for nucleation and growth of the colloidal crystals. After 6−8 h, all MA dispersions showed narrow peaks in UV−visible spectra with percent transmission (%T) at the wavelength of minimum transmittance (λ_{min}) between 582 and 528 nm depending on particle concentration. Since these crystals have weak interparticle interactions, the cells were handled carefully to minimize external forces[3,6,13] that could disrupt the crystals. Iridescence from colloidal crystals was observed within 1−2 min after filling 264 μm thick cells. As the colloidal crystals developed, the %T and the bandwidths decreased. Figure 1 shows UV−visible transmission spectra of the dispersions, and

(15) Haacke, G.; Panzer, H. P.; Magliocco, L. G.; Asher, S. A. U.S. Patent 5,266,238, 1993.
(16) (a) Stöber, W.; Fink, A.; Bohn, E. *J. Colloid Interface Sci.* **1968**, *26*, 62. (b) Bogush, G. H.; Tracy, M. A.; Zukoski, C. F. *J. Non-Cryst. Solids* **1988**, *104*, 95. (c) Badley, R. D.; Ford, W. T.; McEnroe, F. J.; Assink, R. A. *Langmuir* **1990,** *6*, 792.
(17) Philipse, A. P.; Vrij, A. *J. Colloid Interface Sci.* **1988**, *128*, 121.
(18) (a) Sunkara H. B.; Jethmalani J. M.; Ford, W. T. *J. Polym. Sci., Polym. Chem. Ed.* **1992**, *30*, 1917. (b) Pusey, P. N.; van Megen, W. *J. Chem. Phys.* **1984**, *80*, 3513. (c) Ackerson, B. J.; Clark, N. A. *J. Phys.* **1981**, *42*, 929. (d) Pecora, R., Ed. *Dynamic Light Scattering-Applications of Photon Correlation Spectroscopy*; Plenum Press: New York, 1985. (e) Nobbmann, U. M.S. thesis, Oklahoma State University, 1991.
(19) Hiltner, P. A.; Papir, Y. S.; Krieger, I. M. *J. Phys. Chem.* **1971**, *75*, 1881.

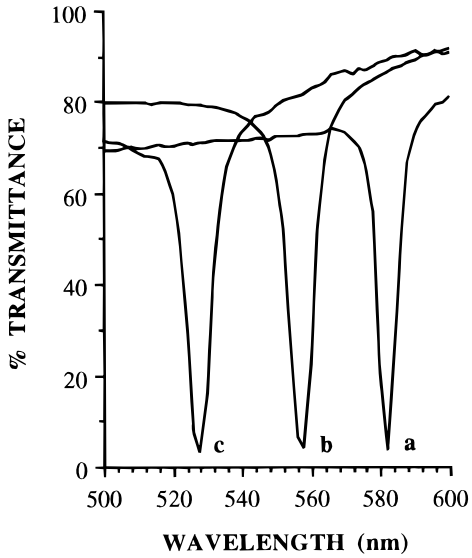

Figure 1. Transmission spectra of 264 μm thick dispersions of 153 nm TPM−silica particles in methyl acrylate: (a) 35, (b) 40, and (c) 45 wt %.

Table 1. Transmission of 153 nm TPM−Silica in MA Dispersions and PMA Composites

	before polymerization		after polymerization	
wt %	λ_{min} (nm)	bandwidth[a] (nm)	λ_{min} (nm)	bandwidth[a] (nm)
35	582	4	502	15
40	556	6	482	13
45	528	6	466	14

[a] The bandwidths were measured at the half-peak height on the absorbance (log I_0/I) scale.

Table 1 gives the measured λ_{min} and bandwidths from the MA dispersions.

The structures of colloidal crystals of silica spheres in ethanol/toluene mixtures at concentrations of 0.344−0.380 g mL^{-1} are reported to be either fcc or a mixture of fcc and hcp (hexagonal close packed).[3b] We observe hexagonal planes of particles parallel to the surface in scanning electron micrographs of polymerized films, which means that the corresponding planes in the TPM−silica−MA dispersions could be 111 planes of fcc or 100 planes of hcp. The d_{111} spacings calculated from transmission spectra using the theory of Bragg diffraction[2,7] for an fcc structure are given in Table 2. The entire 20 × 70 × 0.264 mm cell showed the same λ_{min} at a given particle concentration using a 9 mm circular spectrophotometer beam profile. For example, a 35 wt % silica MA dispersion showed λ_{min} between 580 and 582 nm at edges, top, center, and bottom of the cell with bandwidths at half-height of 4−6 nm. These bandwidths are slightly larger than the values of 3−4 nm calculated theoretically by dynamical diffraction theory using eq (15) in ref 7b.

Scheme 2

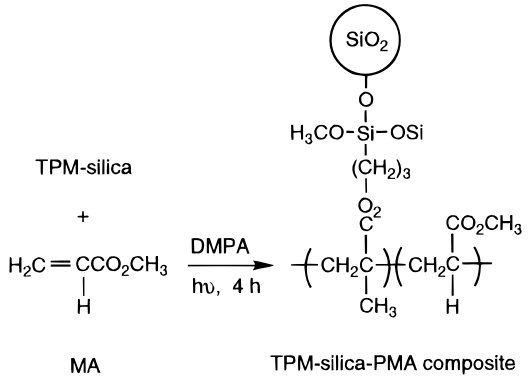

By optical microscopy, no light normal to the cell was transmitted through the MA dispersions between crossed polarizers due to crystal planes parallel to the cell plane.[2,6,19] Upon rotation of the cells 40−55°, brilliant blue and green colored 50−200 μm crystallites appeared throughout the cell. The crystallites were smaller in 45 than in 35 wt % dispersions.

We have also ordered 142 and 330 nm TPM−silica particles in MA dispersions. A 40 wt % 142 nm TPM−silica MA dispersion shows a 4 nm wide %T band with λ_{min} at 490 nm, while a 40 wt % 330 nm TPM−silica MA dispersion shows a 35−50 nm wide band at 600 nm. Increasing the particle size leads to greater scattering of light and broader peaks, as previously observed with polystyrene spheres in water.[7]

PMA Composite. After 6−8 h to develop the colloidal crystals, MA dispersions containing 0.2 wt % DMPA were irradiated using a medium-pressure Hg lamp.[2] Copolymerization of the TPM groups on silica and the MA yields the composite as shown in Scheme 2. The transmission bandwidths of the polymerized composites increased with increasing initiator concentration in the range 0.2−5.0%. Figure 2 shows the transmission spectra from 35, 40, and 45 wt % TPM−silica in PMA composite films, and Table 1 reports λ_{min} values and bandwidths. The d_{111} spacings calculated using the theory of Bragg diffraction[2,7] from transmission spectra of the PMA composites are given in Table 2. On photopolymerization, (a) λ_{min} shifted to the blue, (b) transmittance at λ_{min} increased, (c) bandwidths increased, and (d) λ_{min} and bandwidths varied from one region to another within a single sample. The λ_{min} values varied 10−20 nm, and the typical bandwidths varied within one sample. The best samples had bandwidths of 8−12 nm throughout, and the worst 8−12 nm in ordered regions and up to 30 nm elsewhere. For comparison, the bandwidths of published spectra of colloidal crystals of polystyrene latexes in polyacrylamide gels are 13−18 nm.[14,15]

Stretching the Composite Film. Figure 3 shows the effect of stretching on the transmission spectra of

Table 2. Properties of MA Dispersions and PMA Composites

	MA dispersion			PMA composite			
wt %	n_s	obsd d_{111}[a] (nm)	calcd d_{111}[b] (nm)	n_s	obsd d_{111}[a] (nm)	calcd d_{111}[c] (nm)	decrease in d_{111} (%)
35	1.4112	206	195	1.4721	171	171	17.3
40	1.4125	197	186	1.4712	164	164	16.8
45	1.4142	187	178	1.4700	159	157	16.0

[a] From the Bragg equation, $\lambda = 2n_s d \sin\theta$, where n_s is the dispersion refractive index. [b] From wt % TPM-silica and assumed fcc structure using eq 3 in ref 2b. [c] Based on observed d spacing of MA dispersion, shrinkage during polymerization, and assumed change in d spacing proportional to thickness of film.

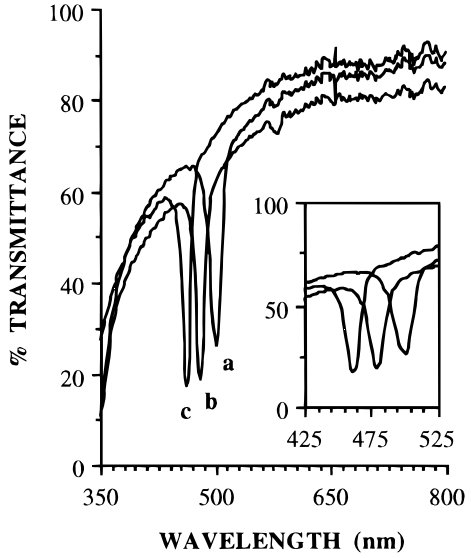

Figure 2. Transmission spectra of 264 μm thick composite films of 153 nm TPM−silica particles in PMA: (a) 35, (b) 40, and (c) 45 wt %.

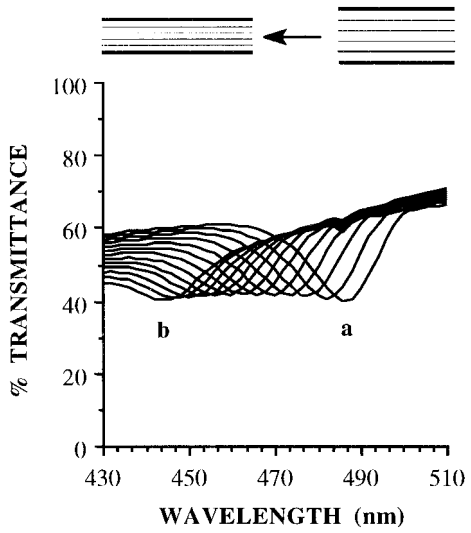

Figure 3. Transmission spectra of 153 nm TPM−silica in PMA (a) before and (b) after uniaxial stretching to $L/L_0 = 1.35$. Intermediate spectra are from the film at $1 < L/L_0 < 1.35$. The initially 228 μm thick film contained 40 wt % TPM−silica.

the 40 wt % TPM−silica−PMA composite. As a film of original length $L_0 = 1.00$ cm was stretched to $L = 1.35$ cm, λ_{min} shifted from 486 nm to 440 nm. With further stretching, the spectral peak became much weaker and broader. Figure 4 shows λ_{min} and bandwidths versus the strain (L/L_0). The 35 and 45 wt % TPM−silica−PMA composite films had similar spectra with blue shifts of λ_{min} from 502 to 448 nm and 466 to 434 nm, respectively, at $L/L_0 = 1.35$. All of the composite films retracted to their original lengths in 2−4 h after releasing the applied stress and showed λ_{min} within 2−4 nm of that observed from the unstretched films. Repeated stretching eventually tore the films.

Swelling the Composite Film. The spectral peak was red-shifted by swelling the composites with monomers such as MA and styrene containing 1 wt % DMPA. Table 3 shows λ_{min} observed from a 40 wt % TPM−silica−PMA composite swollen with MA, Table 4 shows similar data from a 35 wt % TPM−silica−PMA composite swollen with styrene, and Figures 5 and 6 show

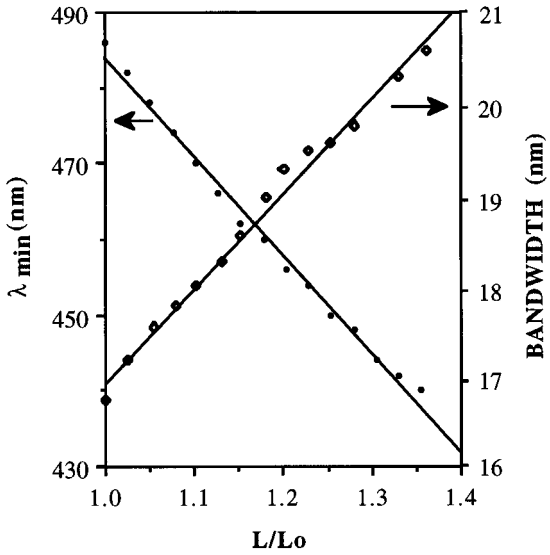

Figure 4. λ_{min} (nm) and bandwidth (nm) versus strain from spectra of Figure 3.

Table 3. Transmission of a 40 wt % 153 nm TPM−Silica in PMA Film Swollen with MA

dimensions (mm)	time (h)	λ_{min} (nm)	obsd d_{111}[a] (nm)	calcd d_{111} (nm)	bandwidth (nm)
70 × 20 × 0.264[b]	0	556	197	186[c]	6
9.0 × 9.0 × 0.228[d]	0	506	172	164[c]	11
11.0 × 11.0 × 0.295[e]	24	652 (655)	226	227[f]	13
10.5 × 10.5 × 0.287[g]	24	632 (637)	214	216[f]	14

[a] Calculated from the Bragg equation. [b] Dimensions of the entire sample of MA dispersion. [c] From Table 2. [d] Dimensions of a piece of the polymerized composite. [e] Swollen with MA and 1 wt % initiator. [f] Calculated from the swollen dimensions of the composite. [g] After photopolymerization. The λ_{min} values in parentheses are calculated from the swollen dimensions of the composite.

Table 4. Transmission of 35 wt % 153 nm TPM−Silica in PMA Film Swollen with Styrene

time (h)	λ_{min} (nm)	bandwidth (nm)
0	502	12
4	680[a]	23
24	740[b]	14
24	724[c]	24
24	550[d]	19

[a] Swollen with styrene. [b] Swollen with styrene and 1 wt % initiator. [c] After photopolymerization. [d] After thermal polymerization of imbibed styrene.

their transmission spectra. Initially diffusion of a band of styrene into the TPM−silica−PMA composite gave a film with two peaks, which at one time appeared at 502 nm for the unswollen region and at 644 nm for the partly swollen region, as shown in spectrum b of Figure 6. After styrene diffused throughout the film, there was only one λ_{min} at 680 nm. From the MA-swollen composite, only one red-shifted peak appeared at 652 nm, and in 2−3 h of swelling, it was weaker than that of the styrene-swollen film. On swelling, the bandwidths increased, and the styrene swollen composite was less transparent than the MA swollen composite at wavelengths away from the λ_{min} due to the greater difference in refractive indexes between the composite and styrene. By swelling, the composite film with initial glass transition temperature (T_g) near room temperature became a gel with a much lower T_g.

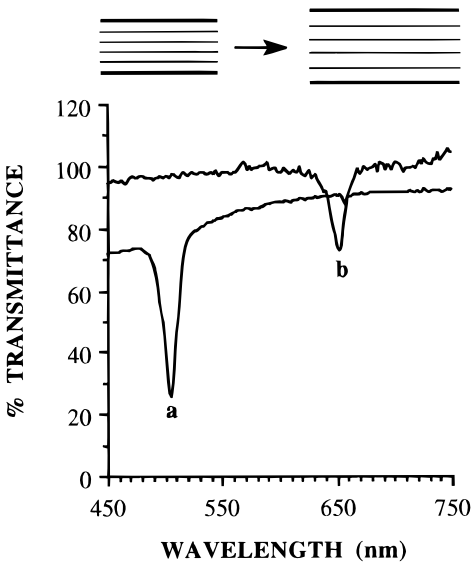

Figure 5. Transmission spectra of 153 nm TPM−silica−PMA composite (a) before and (b) after swelling with methyl acrylate. Before swelling the film contained 40 wt % TPM−silica and was 228 μm thick.

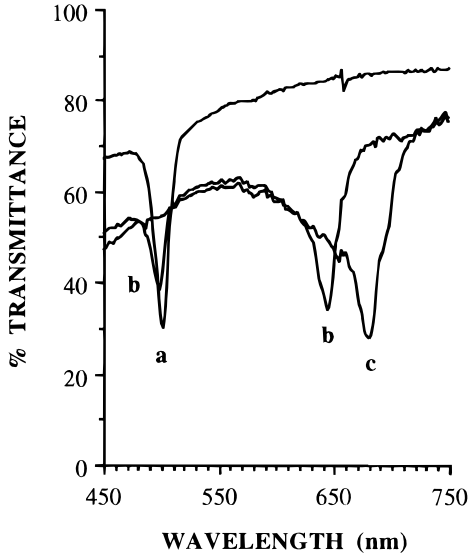

Figure 6. Transmission spectra of a 153 nm TPM−silica−PMA composite film swollen with styrene after (a) 0, (b) 2, and (c) 4 h. Before swelling the film contained 35 wt % TPM−silica and was 228 μm thick.

After 6−8 h, the composite films were allowed to swell further with MA and styrene containing 1 wt % DMPA. During this second period, the fully swollen size of the TPM−silica-cross-linked film was reached, and λ_{min} of the styrene-swollen film increased from 680 to 740 nm. After irradiation for 3−4 h, polymerization of the MA-swollen film was complete, while that of the styrene-swollen film was incomplete resulting in a gel. Heating at 90 °C evaporated the remaining styrene. Figures 7 and 8 show the transmission spectra before and after photopolymerization of the 35 wt % TPM−silica−PMA composites swollen with MA and styrene, respectively. The thickness, length, and width of the sample before and after swelling with MA and photopolymerization are reported in Table 3. The λ_{min} at 506 nm from an unswollen PMA composite film of thickness 228 μm was red-shifted to 632 nm after swelling with MA and further polymerization to a thickness of 287 μm. Figure

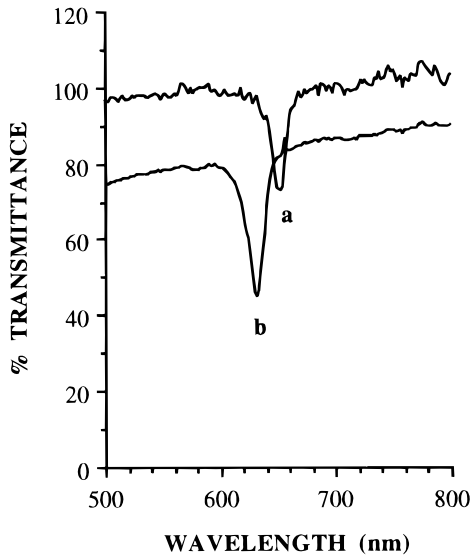

Figure 7. Transmission spectra of a 153 nm, 35 wt % TPM−silica−PMA composite swollen with methyl acrylate (a) before and (b) after polymerization.

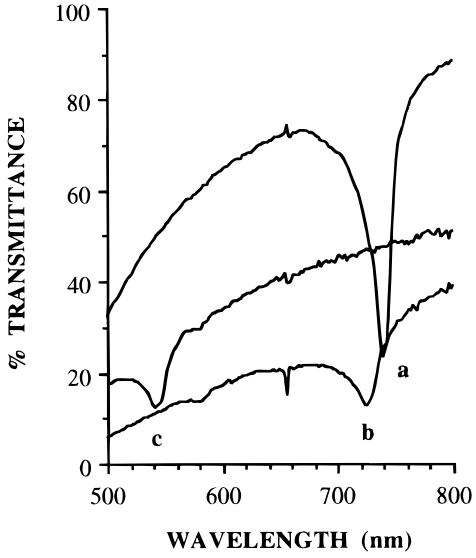

Figure 8. Transmission spectra of a 153 nm, 35 wt % TPM−silica−PMA composite swollen with styrene (a) before and (b) after photopolymerization and (c) after heating at 90 °C.

9 illustrates the dimensional changes of the composite film from photopolymerization, swelling, and photopolymerization of the imbibed monomer. No macroscopic or microscopic phase separation was observed in orthoscopic images of the new composite between crossed polarizers. Figure 10 shows the orthoscopic images of composite films held at an angle of 40−55° from the incident light before and after swelling.[2,6,8] No light was transmitted normal to the film plane, indicating that crystal planes were parallel to the film plane. The dimensions of the crystals were 50−200 μm. The varied colors of the swollen composite are probably due to varied crystal orientations. The regions transmitting no light in Figure 10 did transmit light at different angles of incidence, which proves that there were colloidal crystals throughout the length and width of film.

Rotating the Composite Film. The λ_{min} shifts by rotating the film away from normal to the incident light of a UV−visible spectrophotometer.[10−12] Figures 11 and

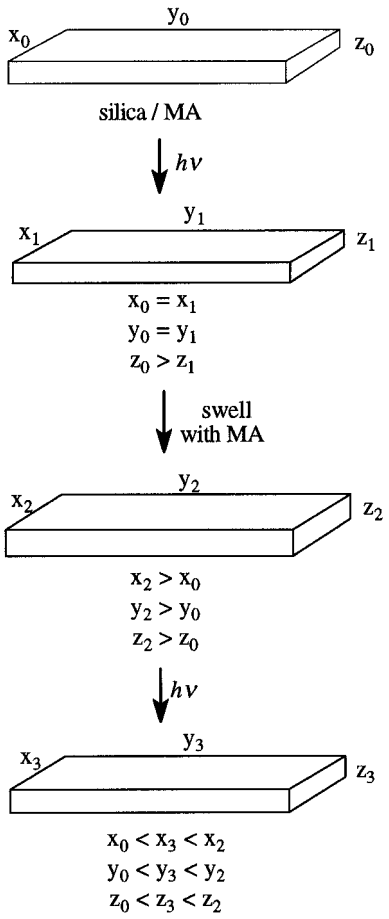

Figure 9. Dimensional changes during photopolymerization, swelling with MA and photopolymerization of imbibed MA of a 40 wt % silica−PMA composite. Measured dimensions are in Table 3.

12 show transmission spectra obtained by rotating a 40 wt % 153 nm TPM-silica in MA dispersion and PMA composite, respectively. Table 5 shows the λ_{min} and spectral bandwidths from a 40 wt % TPM−silica−MA dispersion and a 40 wt % TPM−silica−PMA composite film with light at different incident angles. Similar results were obtained from 35 and 45 wt % TPM−silica PMA composite films. The shifts of λ_{min} are consistent with the Bragg eq 1 and the angle of incidence from Snell's law of refraction:

$$\theta = \cos^{-1}[(\cos \theta_1)/n] \qquad (2)$$

where θ is the corrected Bragg angle, θ_1 is the observed glancing angle, and n is the refractive index of the dispersion or the polymer composite, as previously observed for polystyrene latexes in water.[12] Figure 13 compares observed and calculated diffraction wavelengths with sin θ for MA dispersion and PMA composite.

SEM Analysis. Figure 14 shows SEM images of the surface layers of 40 wt % TPM−silica particles in the unswollen PMA film and the MA-swollen, repolymerized PMA composite film. Figure 14b shows two planes of particles, and only the lower plane contains the complete number of particles of a hexagonal plane. The films were microtomed normal to the film plane, and SEM images of the microtomed surfaces are in Figure 15. The film surface has regular hexagonal arrays of silica particles similar to those observed by SEM of the surface

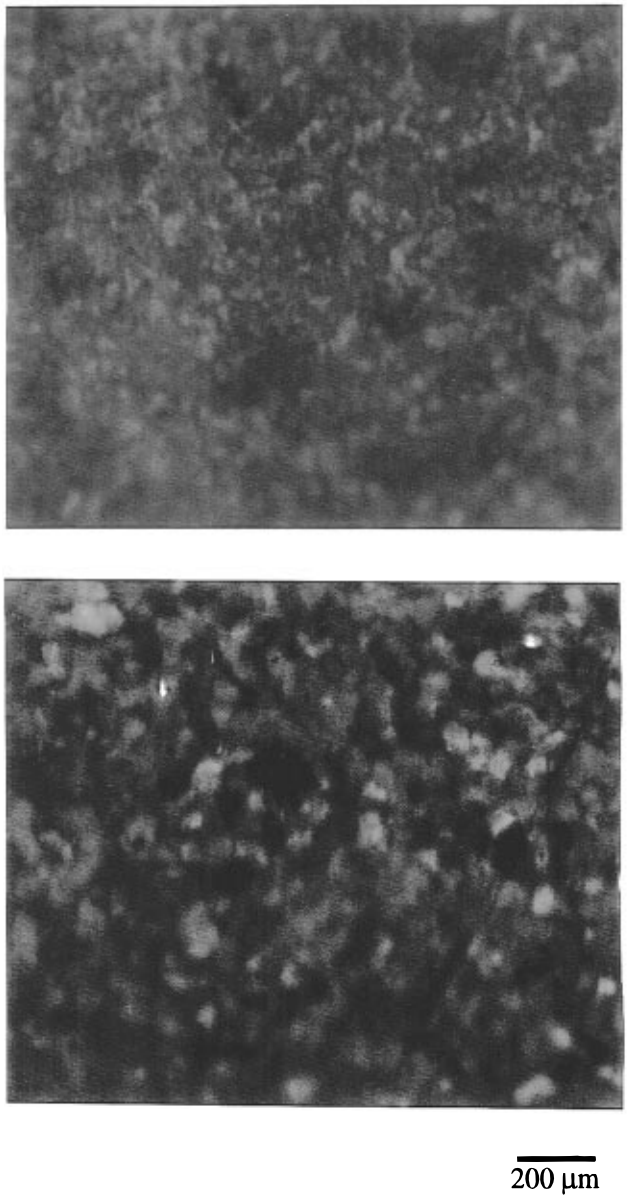

Figure 10. Orthoscopic images of a 153 nm TPM−silica−PMA composite film tilted 40−55° to the incident light between crossed polarizers before (top) and after (bottom) swelling with methyl acrylate.

layer of TPM−silica in a PMMA composite film,[2] and by freeze fracture electron microscopy of polystyrene latexes in hydrogels.[20]

Discussion

Analogy to previous colloidal crystals formed from high concentrations of silica particles with low surface charge[3b] suggests that the 35−45 wt % TPM−silica particles in MA dispersions crystallize into fcc lattices. Wavelengths and bandwidths of peaks in visible spectra fit diffraction theory for fcc d_{111}, hcp 100, or a mixture of fcc and hcp planes parallel to the surface of the glass cells.[2,7,10−15]

After photopolymerizing the monomer dispersions, visible spectra of the composite films indicate that

(20) (a) Goodwin, J. W.; Ottewill, R. H.; Parentich, A. *J. Phys. Chem.* **1986**, *84*, 1580. (b) Cohen, J. A.; Scales, D. J.; Ou-Yang, H. D.; Chaikin, P. M. *J. Colloid Interface Sci.* **1993**, *156*, 137. (c) Kamenetzky, E. A.; Magliocco, L. G.; Panzer, H. P. *Science* **1994,** *264*, 207.

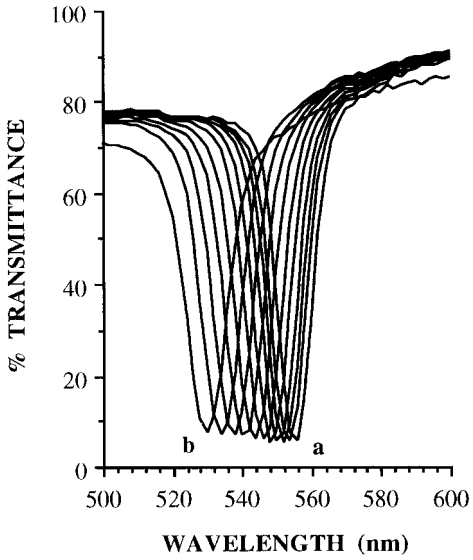

Figure 11. Transmission spectra of a 40 wt % 153 nm TPM−silica in MA dispersion as a function of angle of incidence: (a) 90° and (b) 66°. Film thickness = 264 μm. Data are in Table 5.

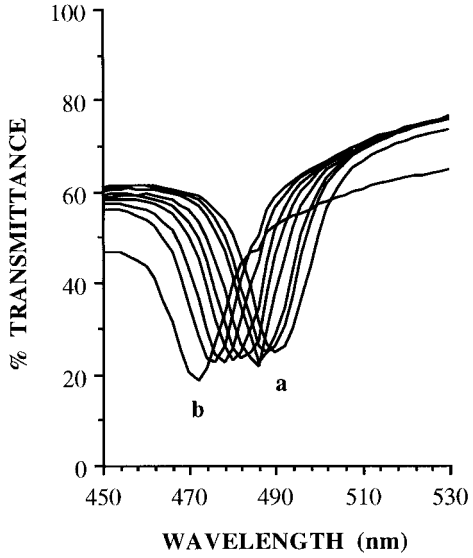

Figure 12. Transmission spectra of 40 wt % 153 nm TPM−silica−PMA composite as a function of angle of incidence: (a) 90° and (b) 68°. Film thickness = 228 μm. Data are in Table 5.

Table 5. Transmission of 40 wt % 153 nm TPM−Silica in MA Dispersion and PMA Composite as a Function of the Glancing Angle, θ_1

	MA dispersion		PMA composite	
θ_1 (deg)	λ_{min} (nm)	bandwidth (nm)	λ_{min} (nm)	bandwidth (nm)
90	556	7	490	14
84	554	8	490	14
82	552	7	488	14
80	550	8	486	13
78	548	8	486	12
76	546	8	482	13
74	544	9	480	13
72	540	9	478	12
70	538	9	476	12
68	534	9	472	11
66	530	9		

crystallinity and the hexagonal planes parallel to the film plane are maintained. A blue-shift of the diffraction wavelength occurs from all of the composite films

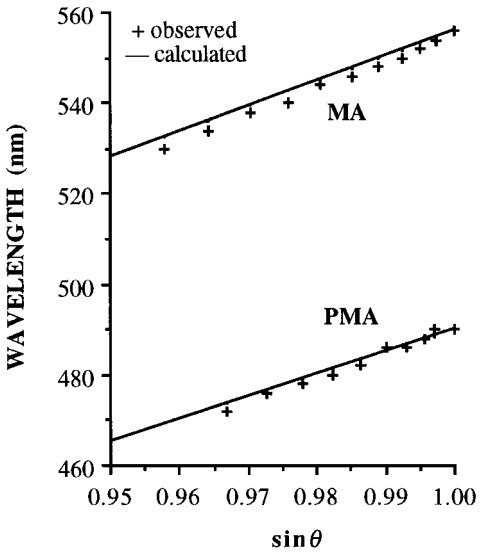

Figure 13. Plot of diffracted wavelength versus sin θ for the MA dispersion and PMA composite given in Table 5.

because of decrease of the film thickness and thus the interplanar spacing.[2] Polymerization of MA to PMA occurs with a decrease in specific volume from 1.046 to 0.820 cm^3 g^{-1}.[21] The shrinkage occurs entirely in the thickness of the film, not in the length or width, because the composite adheres to the epoxy used to seal the sandwiched glass slides and not to the poly(dimethylsiloxane)-coated glass surface. Assuming affine deformation, if the crystals are fcc in the monomer dispersion, shrinking only normal to the d_{111} plane leaves a rhombohedral structure, or if the crystals are hcp in the monomer dispersion, shrinking leaves a more compressed hcp structure in the polymer film.

The *d* spacings calculated from transmission spectra of the silica−PMA films are in good agreement with the *d* spacings calculated by assuming monomer shrinkage only in the film thickness, as seen in Table 2. The λ_{min} of the polymerized film varies from one region to another probably due to nonuniform decrease in thickness, such that thinner regions have smaller *d* spacing than thicker ones. The intensities of the diffraction peaks of the composite are less than those of the MA dispersion in part due to a smaller refractive index difference between the silica and the matrix. The broader bandwidth from the composite is primarily due to decrease of inter- and intracrystalline order during photopolymerization.

With an increase of the particle concentration from 35 to 45 wt %, the crystal cell dimensions decrease, and the decrease of *d* spacing causes a blue-shift of the diffraction wavelength from the monomer dispersions and the polymer films. The blue-shift is similar to that observed from colloidal crystals of silica in ethanol/toluene or polystyrene latexes in water.[3,6−8,13]

The blue shift of λ_{min} in Figure 3 indicates that the *d* spacing of the colloidal crystal decreases as the films are stretched uniaxially to $L/L_0 = 1.35$. On further stretching, severe broadening of the spectral peaks suggests that either the uniform orientation of the crystallites or the order within the crystallites deteriorates.[14] Similarly, even at $1 < L/L_0 \leq 1.35$, the increase

(21) Scientific Polymer Products, Inc., Catalog, Ontario, New York, 1991−92.

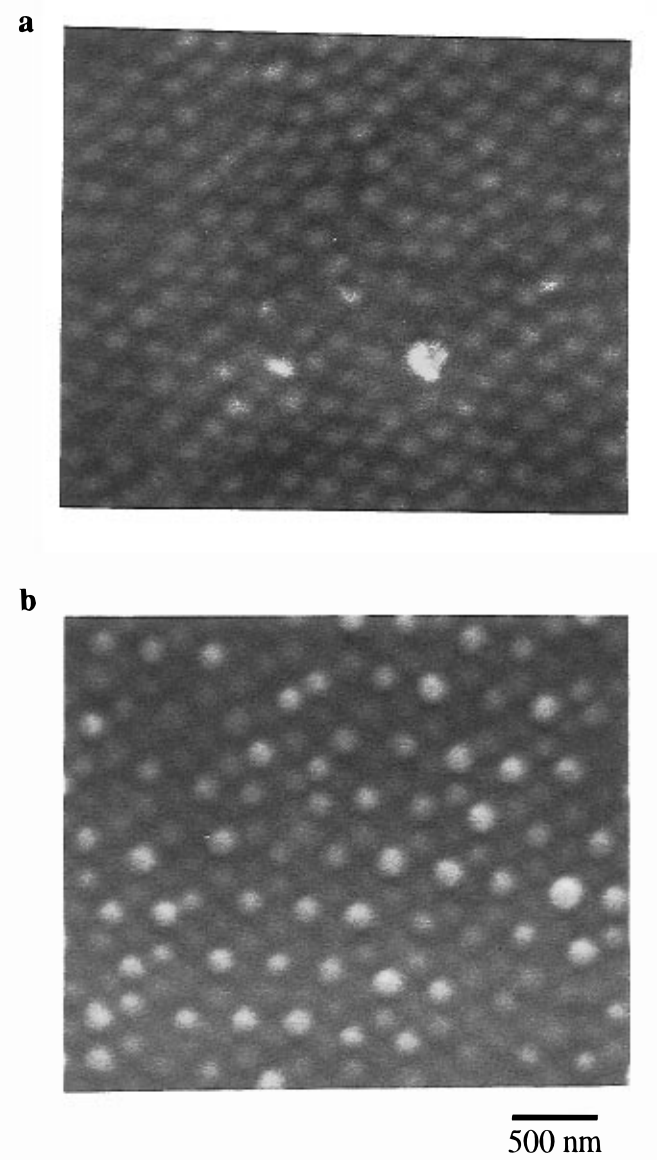

Figure 14. SEM image of a surface layer of a 40 wt % 153 nm TPM−silica−PMA composite film (a) before and (b) after swelling and photopolymerization of MA. Film thickness = 228 μm before swelling and 287 μm after second polymerization.

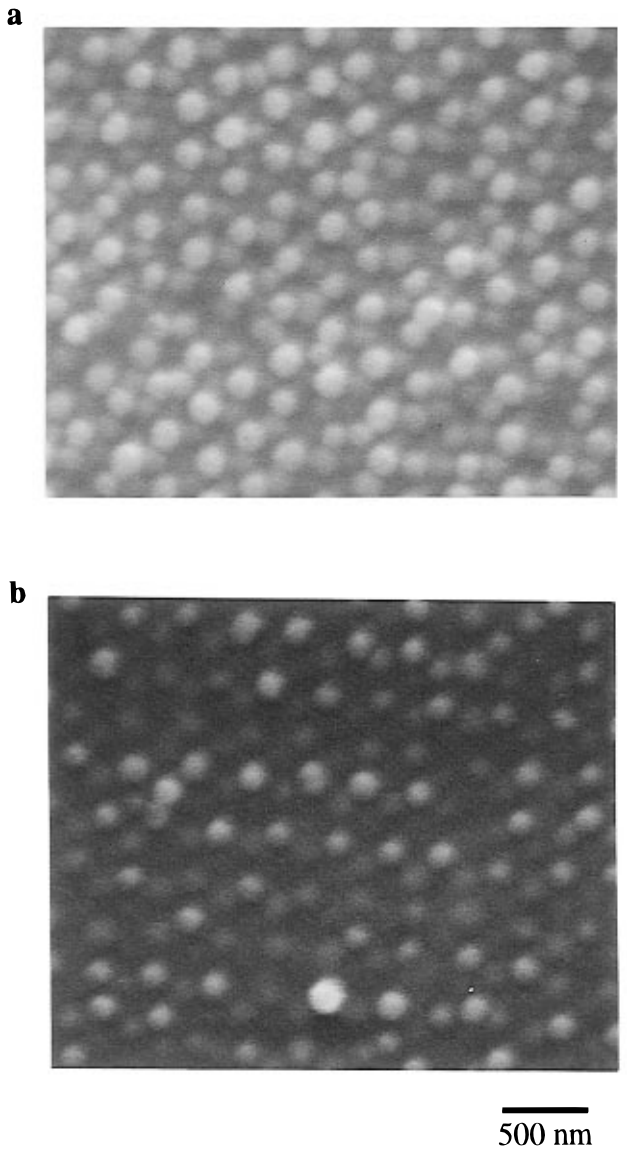

Figure 15. SEM image of a microtomed section of a 40 wt % 153 nm TPM−silica−PMA composite film (a) before and (b) after swelling and photopolymerization of MA. Film thicknesses are the same as in Figure 14.

of the bandwidth is probably due to decrease of inter- or intracrystalline order. As long as the film of 40 weight percent silica in PMA is not stretched to $L/L_o > 1.35$, it behaves as an elastomer with a very slow recovery, regaining its macroscopic dimensions and its crystal dimensions, as measured by visible spectra, within 4 h after releasing the stress. These silica−PMA composites provide convenient control of the diffraction wavelength by stretching and are mechanically stronger than polyacrylamide gels containing polystyrene latexes.[14,15]

We have not been able to grow colloidal crystals of 153 nm monodisperse silica in MA or MMA at concentrations of less than 35 wt %, and consequently the diffraction wavelengths of the initially polymerized films are limited to ≤510 nm. This problem has been solved by swelling colloidal crystalline silica−PMA films with more monomer. The crystalline order is retained, and polymerization of the imbibed monomer gives a robust film with $\lambda_{min} = 632$ nm as shown in Figure 7. The red-shifts of λ_{min} in the spectra of Figures 5−8 show that swelling the composite matrix with MA or styrene increases the d spacings of the crystal lattice. The d spacing of 226 nm calculated from the Bragg equation and λ_{min} of the MA swollen composite agrees well with the d spacing of 227 nm calculated from the thickness of the film assuming affine swelling of the crystal lattice.

On photopolymerization of added monomers, blue-shifts of diffraction wavelengths are due to shrinkage of the thickness of the composite as discussed above. The agreement between d spacing of 214 nm calculated from transmission spectra and $d = 216$ nm calculated from the film thickness indicates that photopolymerization shrinks the swollen crystal lattice in proportion to the polymer matrix.

Since the films between crossed polarizers are not birefringent to light normal to the surface and blue-green crystallites appear when the film is tilted 40−55°, the lattice plane causing diffraction is parallel to the plane of the glass, as observed previously with a silica−PMMA composite.[2] The shift of diffraction from blue-green to red through crossed polarizers when the polymer composite swells is due to the increased d

spacing, but the multicolored image of Figure 10b shows that not all of the crystal planes are parallel to the surface. The hexagonal order observed in the SEM images of the surface layer and the microtomed layer also indicates that planes of the crystals in Figures 14 and 15 are parallel to the film plane and that the particle order is trapped by photopolymerization.[2,20]

The tuning of diffraction wavelengths of a silica−PMA film by stretching and swelling is due to its elastomeric properties. The PMA matrix is linked to the silica particles by copolymerization with the methacrylate groups of the silane coupling agent TPM, so that the silica effectively acts as a cross-linker. This prevents the polymer film from dissolving in more monomer and provides the elastic force to restore the stretched film to its original dimensions after stress is released.

Acknowledgment. This research was supported by National Science Foundation Grant DMR-9503626. We thank Bruce J. Ackerson and Hari Babu Sunkara for helpful discussions and Ginger Baker for technical help with scanning electron microscopic analysis.

CM960065U